# Ratio of Vacancy Jump Frequencies around and away from Copper Impurity Atoms in Aluminum

T. R. Anthony

*General Electric Research and Development Center, Schenectady, New York* 12301

(Received 19 February 1970)

During the precipitation of a supersaturated solution of vacancies in a dilute aluminum-copper alloy, large vacancy condensation cavities are formed at the metal-oxide interface of the alloy. The vacancy current that produced these cavities was directly determined from the cavity volume. A microprobe examination in and around the cavities determined the copper impurity current which had been generated by the vacancy current forming these cavities. From the values of the vacancy and copper impurity currents found in the experiment, the ratio of the jump frequency of a vacancy away from a copper impurity atom to that around a copper impurity atom is calculated. This ratio suggests a very small binding between a vacancy and a copper impurity and/or a slight increase in the jump frequency of solvent atoms next to the undersized copper impurity.

## I. INTRODUCTION

Recently, jump frequencies of vacancies in the neighborhood of impurity atoms in fcc metals have been successfully computed from experimental measurements[1,2] of the correlation coefficient for impurity diffusion, the impurity diffusivity, the solvent diffusivity, and the effect of solute concentration on the solvent diffusivity by utilizing a theory based on nearest-neighbor interactions.[3] The purpose of this paper is to describe a new experiment which allows one to determine the ratio of the vacancy jump frequencies away from and around an impurity atom in some cases and limits of this ratio in all other cases. This experiment involves the direct measurement of the impurity current that is generated by a vacancy current in a metal.

## II. IMPURITY CURRENT GENERATED BY A VACANCY CURRENT

Consider a dilute alloy containing solvent atoms $A$, solute (impurity) atoms $B$, and vacancies $V$. The currents $J_A$, $J_B$, and $J_V$ of atoms $A$ and $B$ and vacancies $V$ under isothermal conditions can be expressed in the notation of irreversible thermodynamics as

$$\begin{aligned} J_A &= L_{AA}X_A + L_{AB}X_B + L_{AV}X_V, \\ J_B &= L_{BA}X_A + L_{BB}X_B + L_{BV}X_V, \\ J_V &= L_{VA}X_A + L_{VB}X_B + L_{VV}X_V, \end{aligned} \tag{1}$$

where the thermodynamic driving forces $X_i$ are the gradients of the chemical potential of the constituents of the solution, and $L_{ij}$ are phenomenological coefficients related to atomic mobilities. Equations (1) state that a current of $A$, $B$, or $V$ is not only generated by its own chemical potential gradient, but also by chemical potential gradients in the other two solution components. Of particular interest in this paper will be the fact that a vacancy potential gradient can cause currents of $A$ and $B$ atoms as well as vacancy currents.

Several factors quickly reduce the apparent complexity of Eqs. (1). First, by a judicious selection,[4,5] the phenomenological coefficients $L_{ij}$ can be made to obey the Onsager relation. Second, Eqs. (1) in their full form are overstated[5] since the Gibbs-Duhem relation and the conservation of lattice sites, respectively, provide additional relations between the thermodynamic forces and the currents.

Both the thermodynamic forces $X_i$ and the phenomenological coefficients $L_{ij}$ are influenced by the formation of impurity-vacancy pairs $P$ in the solution. The concentration of impurity-vacancy pairs is expressed in the following mass action relation describing the interaction between vacancies, impurity atoms, and impurity-vacancy pairs in the solution[6]:

$$C_p = (C_v - C_p)(C_B - C_p)K. \tag{2}$$

Here $C_p$ is the atomic fraction of impurity-vacancy pairs, $C_B$ is the total atomic fraction of the impurity, and $C_v$ is the total atomic fraction of vacancies (including those vacancies contained in pairs).

Howard and Lidiard[7] have calculated the chemical potentials of the alloy constituents $A$, $B$, and $V$ by considering the configurational entropy that results from the distribution of solvent $A$, impurity $B$, vacancies $V$, and solute-vacancy pairs $p$ over all sites of the crystal lattice. Using these chemical potentials and all of the information mentioned above, they calculated the impurity current $J_B$ correct to the first order in $C_B$ to be

$$\begin{aligned} J_B = &[kT(L_{BA} + L_{BB})\nabla \ln(C_v - C_p)] \\ &- [kT(L_{BB})\nabla \ln(C_B - C_p)] \quad . \end{aligned} \tag{3}$$

The first term in Eq. (4) is the impurity current that results from a gradient in the free-vacancy concentration and is the term that will be of particular interest in this paper. The second term in Eq. (4) describes the more familar impurity flow that is caused by an impurity concentration gradient. If one begins with an initially homogeneous alloy ($\nabla C_B = 0$), this second term will simply tend to buffer any buildup in either direction of a solute gradient produced by the first term. For an alloy in which a gradient in the free-vacancy concentration generates only a small or negligible impurity gradient, this second term may be ignored. As will be seen in Sec. III, this situation is in accord with the experimental results reported in this paper.

Assuming an impurity content much larger than the vacancy concentration ($C_B \gg C_V$), one can show that the currents of impurity atoms and vacancies are[7]

$$J_B = \frac{N\nabla C_V K C_B D_P}{1+KC_B}\,\frac{L_{BA}+L_{BB}}{L_{BB}}\,, \qquad J_V = -N\nabla C_V\,\frac{D_V+KC_BD_P}{1+KC_B}\,, \tag{4}$$

where $D_V$ and $D_P$ are the diffusion coefficients of free vacancies and pairs, respectively. The sign convention assumed here is that a flux $J_i$ is positive when the flow is away from a vacancy sink, and negative when the flow is towards a vacancy sink with respect to the local lattice. The ratio of the impurity current generated by the vacancy current ($J_B/J_V$) can be obtained from Eqs. (4) yielding

$$\frac{J_B}{J_V} = -\frac{KC_BD_P}{D_V+KC_BD_P}\,\frac{L_{BA}+L_{BB}}{L_{BB}}\,. \tag{5}$$

The free-vacancy diffusion coefficient $D_V$ in the solution can be written in terms of the self-diffusion coefficient $D_A$ of the pure solvent $A$,

$$D_A = (C_V - C_P)D_V. \tag{6}$$

Note that $(C_V - C_P)$ is the atom fraction of free vacancies in the dilute solution and is equal to a first-order approximation to the total atom fraction of vacancies in the pure solvent at the same temperature. In addition, the pair diffusion coefficient $D_P$ can be expressed in terms of the diffusion coefficient $D_B$ of impurity $B$ in solvent $A$ and the ratio of the pair concentration $C_P$ to the total impurity concentration $C_B$:

$$D_B = (C_P/C_B)D_P. \tag{7}$$

Equation (7) simply expresses the fact that only an impurity atom with a vacancy as a nearest neighbor can make a displacement jump in a substitutional solution.[8] Finally, for an impurity concentration much larger than the vacancy concentration ($C_B \gg C_V$, therefore $C_B \gg C_P$), the mass action relation between pairs, vacancies, and impurity atoms becomes[9]

$$C_P/C_B(C_V - C_P) = K. \tag{8}$$

Introducing Eqs. (6)–(8) into Eq. (5), we have[10]

$$\frac{J_B}{J_V} = -\frac{C_BD_B}{D_A+C_BD_B}\,\frac{L_{BA}+L_{BB}}{L_{BB}}\,. \tag{9}$$

For the special case of an fcc alloy, Howard and Lidiard,[11] using an atomistic model restricted to nearest-neighbor interactions, have calculated expressions for the phenomenological coefficients $L_{AB}$ and $L_{BB}$ in terms of the various vacancy jumping frequencies in a dilute solution. If $W_1$ is the jumping frequency of a vacancy from one nearest-neighbor position of an impurity to another (Fig. 1), and $W_3$ is the jumping frequency of the vacancy away from the impurity (thereby breaking apart the impurity-vacancy pair), Eq. (9) becomes

$$\frac{J_B}{J_V} = \frac{C_BD_B}{D_A+C_BD_B}\,\frac{W_1 - \frac{13}{2}W_3}{W_1+\frac{7}{2}W_3}\,, \tag{10}$$

where $C_B \gg C_V$ and $\nabla C_B \approx 0$. Solving for the vacancy jump frequency ratio of $W_3/W_1$, we find that

$$W_3/W_1 = (1-\phi)\left(\tfrac{13}{2}+\tfrac{7}{2}\phi\right)^{-1}\,, \tag{11}$$

where

$$\phi = (J_B/J_V)[(D_A+C_BD_B)/C_BD_B]\,. \tag{12}$$

From Eq. (11) and (12), one can see that measurements of the self-diffusion coefficient of the matrix metal $D_A$, the impurity diffusion coefficient $D_B$, and the impurity current $J_B$ generated by a vacancy

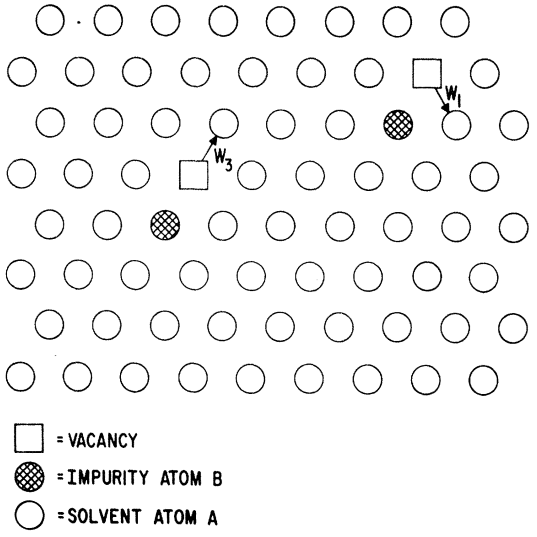


FIG. 1. Vacancy jump frequencies away from ($W_3$) and around ($W_1$) impurity atoms in a dilute alloy.

current $J_V$ will allow one to calculate the ratio of vacancy jump frequencies around and away from impurity atoms in fcc metals in which only small impurity gradients are produced. In other cases where the vacancy current generates large impurity gradients, a limit of this ratio $W_3/W_1$ can be computed.[10]

## III. EXPERIMENTAL PROCEDURE

### A. Selection of Materials

Aluminum was selected as the matrix material for three reasons. First, aluminum has an fcc structure. Second, such parameters as impurity diffusivities[12-24] and the self-diffusivity[25-27] have been well characterized in earlier investigations. Finally, large vacancy condensation cavities form immediately beneath the oxide skin of aluminum during cooling from a high-temperature anneal.[28-37] The final size of these cavities allows one to measure directly the total vacancy current that formed them during cooling.[10]

The impurity current that was generated by the vacancy current forming these cavities can be determined from the change in impurity concentration that occurs around the vacancy condensation cavities. Copper was selected as the impurity additive for several reasons. First, the electron microprobe is capable of detecting small amounts of copper in aluminum. Second, the relatively large solubility of copper in aluminum, in the temperature range in which vacancy condensation cavities form, eliminates copper precipitation during pit formation. Finally, the small atomic size and low valence of copper relative to aluminum makes the vacancy jump frequencies around a copper impurity atom of particular interest.

### B. Specimen Preparation

There were 200 g of an aluminum-copper alloy (0.21-at.% copper) prepared from 99.9999% aluminum and 99.999% copper. Under one atmosphere of argon, the alloy was melted in a degassed graphite crucible, homogenized by mechanical agitation, and finally poured into a graphite mold. The resulting $1.2 \times 5 \times 7.5$-cm ingot was annealed at 630 °C for 5 days, air cooled, and rolled down to a sheet thickness of 0.3 cm. From this sheet, specimens of $2.5 \times 1.2 \times 0.3$ cm were cut. The surface layer of these specimens was removed by etching in aqua regia in order to eliminate any surface impurities acquired during the rolling operation. The specimens were then reannealed for three days at 630 °C and air cooled to room temperature. One face of the specimen was ground and polished using successively finer grades of an aluminum oxide abrasive. Finally, the ground face of the specimen was electropolished in a solution of 80% absolute methanol and 20% perchloric acid maintained at 0 °C. Polishing was conducted at 20 V with a surface current density of 1.2 A/cm$^2$ for approximately 10 min. Following electropolishing, the samples were washed in fresh absolute methanol, rinsed in a jet of distilled water for one minute, and dried with a blast of compressed air.

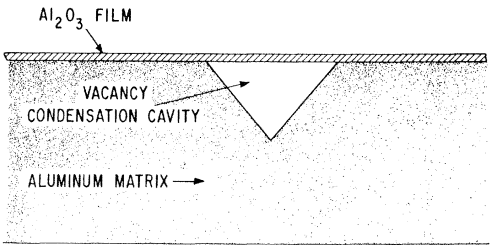


FIG. 2. Vacancy condensation cavity beneath the $Al_2O_3$ film formed by cooling the dilute aluminum-copper alloy from near its melting point.

The electropolished specimens were placed in an annealing furnace open to the atmosphere and heated for 3 h at 630 °C. After this anneal, the specimens were cooled at a rate of 0.12 °C/sec to 400 °C and air cooled to room temperature. During cooling, vacancies precipitated from the supersaturated solution produced by the temperature decrease, forming vacancy condensation cavities at the metal-oxide interface[10, 28-37] of the aluminum-copper alloy (Fig. 2). The particular cooling rate of 0.12 °C/sec was empirically selected in order to produce large vacancy condensation cavities. This relatively slow cooling rate also had the advantage that large concentration gradients in vacancies could not develop during cavity growth, therefore, the theory developed earlier in this paper is applicable. Finally, because of the strong exponential decrease of the equilibrium vacancy concentration with temperature,[38] practically the entire vacancy current which created the vacancy condensation cavities occurred during the first 100 °C decrease from the 630 °C annealing temperature. Consequently, the vacancy and copper impurity currents that are determined in this experiment will be temperature-averaged values for the 630–530 °C temperature range.

## IV. EXPERIMENTAL RESULTS

### A. Vacancy Current

The total vacancy current that generated the vacancy condensation cavity can be directly determined from the cavity volume $V_C$. Figure 3 shows a schematic diagram of a vacancy cavity beneath the aluminum oxide film. For the moment, let $S$ be the area of a surface enclosing the aluminum

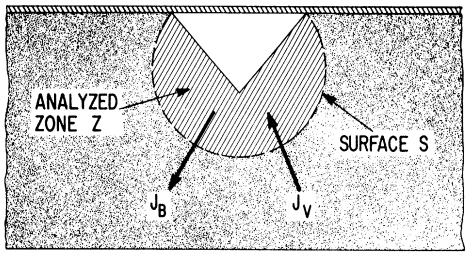


FIG. 3. Vacancy condensation cavity in aluminum showing the zone analyzed by the electron microprobe, the vacancy current, and the copper impurity current generated by the vacancy current.

matrix around the vacancy cavity. Then we can write

$$\int_{\text{time}} J_V S dt = V_C, \tag{13}$$

where $t$ is the variable in time and $V_C$ is the volume of the vacancy condensation cavity. Since the thin (120 Å) $Al_2O_3$ film over the cavity is transparent in the optical region, both the shape and depth of the pit were determined from the displacement of interference fringes viewed in an optical interference microscope. In this manner, the cavity volume was directly determined.

### B. Impurity Current Generated by Vacancy Current

The region $Z$ in Fig. 3 is the alloy volume analyzed by the electron microprobe. For determinations of small copper concentrations in aluminum, the size of this analyzed zone is not limited by Cu $K\alpha_1$ x-ray absorption, but is instead defined by the effective electron scattering length which in aluminum is approximately 5 $\mu$ for the microprobe accelerating voltage used in these experiments.

The total impurity flow through the surface $S$ induced by the vacancy flow can be computed from the vacancy-cavity volume $V_C$, the analyzed-zone volume $V_Z$, and the concentration change in the analyzed zone from the original impurity level. Thus we have

$$\int_{\text{time}} J_B S\, dt = -C_B^0 V_C - (C_B^0 - C_B) V_Z, \tag{14}$$

where $C_B^0$ is the original impurity concentration and $C_B$ is the impurity concentration in the analyzed zone following the growth of the vacancy condensation cavity.

There are several experimental problems associated with determining the concentration change $(C_B^0 - C_B)$ around the vacancy condensation cavity with the electron microprobe. First, one must establish $C_B^0$ in the area of the vacancy cavity since long-range impurity gradients in the specimen may cause the initial impurity concentration around the cavity to differ from the average nominal impurity concentration of the specimen. This problem is easily solved by determining the impurity concentration 50 $\mu$ away from the cavity on the free surface. The composition at this position will be typical of the local initial impurity concentration and is far enough away from the vacancy cavity so as to be unaffected by the vacancy currents which produce the vacancy cavity. Thus, the comparison of the impurity concentration here with that in the vacancy condensation cavity makes an accurate measurement of $(C_B^0 - C_B)$ possible.

However, comparing the impurity concentration on the free surface with that in the cavity generates two additional problems. First, the percentage of electrons of the impinging electron microprobe beam that are backscattered is expected to change when the beam is moved from a free-surface position to the middle of the vacancy cavity. Since these backscattered electrons do not contribute to the generation of x rays from the impurity atoms, a change in the x-ray intensity may occur without a parallel change in impurity concentration. A solution to this problem is to normalize the x-ray intensity for any fluctuations in backscattered electrons. This normalization is easily accomplished by monitoring the specimen current, which is a direct measure of the number of electrons actually penetrating into the specimen. In the present experiments, this correction amounted to less than 3%.

The second problem associated with the electron mircroprobe analysis is the difference in x-ray absorption for analysis carried out in the vacancy cavity as opposed to the free surface. Fortunately, this problem is minimized in the detection of copper in aluminum because of the low absorption coefficient of the aluminum matrix for Cu $K\alpha_1$ x rays. Nevertheless, the following sequence of steps was used to solve empirically the complicated problem of the effect of the cavity geometry on the intensity of the Cu $K\alpha_1$ line. (i) The intensity of the Cu $K\alpha_1$ line was determined on the free surface 50 $\mu$ away from the cavity of interest. (ii) The intensity of the Cu $K\alpha_1$ line was determined in the cavity. (iii) Without moving the microprobe beam from its position in (ii) the white radiation backgrounds at wavelengths adjacent to and on both the high and low wavelength sides of the Cu $K\alpha_1$ line were determined. (iv) The white radiation backgrounds at the same wavelengths used in (iii) were determined at the initial free-surface position of (i). It should be emphasized here that the Cu $K\alpha_1$ intensity was recorded both on the free surface (i) and in the cavity (ii) without a change in spectrometer setting, because of the sensitivity of the Cu $K\alpha_1$ line to the exact spectrometer setting. The reasons for the rest of the procedure will be

explained below.

At any given x-ray wavelength, the real intensity of the continuous white radiation background in the cavity should be equal to that outside the cavity since the sample is essentially pure aluminum in both spots. Thus, any measured difference in white radiation background is attributable to geometric effects of the cavity. Since the average value of the two wavelengths of the white radiation background that were examined is the same wavelength as the Cu $K\alpha_1$ line, it is expected that the effects of the cavity geometry on the intensity of the Cu $K\alpha_1$ line will be the same as those on the average value of the white radiation background. Consequently, provided that both the copper and background intensities are measured in the same position in the cavity, one can then normalize the Cu $K\alpha_1$ intensity in the cavity to a free-surface value from knowing how the background in the cavity is changed from its free-surface value. It was for this reason that the position of the microprobe beam was carefully left unchanged between (ii) and (iii). In each case, this absorption correction for the cavity geometry amounted to less than 3%.

The actual microprobe examination was performed with a C.E.C. Cameca microprobe. Four different vacancy cavities were examined, each having a size of approximately $9 \times 9$ $\mu$ by 2 $\mu$ deep. The impinging microprobe beam, which had a diameter of about 1.5 $\mu$ fit easily into the vacancy cavities. The background and Cu $K\alpha_1$ intensities were counted for 10 min each for in-cavity and free-surface positions. Table I shows the Cu $K\alpha_1$ line intensity adjusted for specimen current and geometric effects of the cavity in counts per minute to a 95% confidence level. This Cu $K\alpha_1$ intensity was three times the white radiation background intensity on either side of the Cu $K\alpha_1$ peak. From Table I, it is apparent that the vacancy current which generated the condensation cavities caused almost no detectable change in the impurity concentration around the cavity.

### C. Vacancy Jump Frequencies

Dividing Eq. (14) by Eq. (13) gives a time-averaged ratio of the vacancy current and the impurity current generated by a vacancy current

$$\langle J_B/J_V\rangle = -C_B^0 - (C_B^0 - C_B)(V_Z/V_C) \quad . \tag{15}$$

Substituting in for values $C_B^0$, $C_B^0 - C_B$, $V_Z$, and $V_C$ determined in the experiment,

$$\langle J_B/J_V\rangle = -C_B^0\,(0.98 \pm .03). \tag{16}$$

Note that the current of copper atoms away from the vacancy cavity is approximately that $(C_B^0)$ expected on the sole basis of the atomic fraction of copper in solution. After substituting this value of the ratio of the impurity and vacancy currents and a temperature-averaged value of the ratio (2.3) of the aluminum self-diffusion coefficient[25] and the copper impurity diffusion coefficient[12] into Eqs. (11) and (12), the ratio of the vacancy jump frequencies $W_3/W_1$ in a dilute aluminum-copper alloy in the temperature range of 530–630 °C is

$$W_3/W_1 = 0.30 \pm 0.02. \tag{17}$$

### D. Discussion

Both size and valence effects are expected to influence the ratio $W_3/W_1$ of the vacancy jump frequencies associated with impurities in fcc metals. An oversized impurity, for example, would tend to limit the mobilities of its solvent nearest neighbors because of local crowding. Consequently, the vacancy jump frequency $W_1$ around an oversized impurity would be restricted. On the other hand, an undersized impurity would permit more freedom of movement for its nearest neighbors, so that in this case $W_1$ would probably increase around an undersized impurity. Thus, in the dilute aluminum-copper alloy used in the experiments described above, one would anticipate some enhancement of $W_1$ since a copper atom is 10% smaller than an aluminum atom.

Size effects may also influence the vacancy jump frequency $W_3$ away from an impurity atom. The lattice strain that results from either an undersized or an oversized impurity atom is partially relieved when a vacancy occupies a nearest-neighbor position of the impurity. This decrease in the strain energy of the lattice is in effect a binding energy between the vacancy and the impurity. Consequently, vacancy jumps away from the impurity ($W_3$) will be resisted in solutions with either over or undersized impurities. Thus, the presence of an undersized impurity atom such as copper in aluminum will tend to decrease $W_3$.

In aluminum, however, a more important factor than atomic size in determining impurity-vacancy binding energies is solute valence.[12,13,39] Impurity-valence effects are usually discussed in terms of $Z$, the valence difference between impurity and solvent atoms. The perturbing potential of the impurity, which is a result of the valence difference $Z$, is screened by the conduction

TABLE I. The Cu $K\alpha_1$ intensity in the cavity and 50 $\mu$ from the cavity adjusted for specimen current and geometric absorption effects of the cavity to a 95% confidence level.

| | In cavity | 50 $\mu$ from cavity |
|---|---|---|
| Cu $K\alpha_1$ | 2020 ± 32 cpm | 1980 ± 32 cpm |

electrons so that the range of influence of this perturbing charge is drastically reduced in a metal. The screening is imperfect in the sense that the screening electrons tend to overshoot and cause positive and negative oscillations in the radial potential away from the impurity. In aluminum, conditions are such that a negative Friedel oscillation caused by the screening overshoot occurs at the first nearest-neighbor position of the impurity.[13,39,40] Thus, the first nearest neighbor of an impurity in aluminum sees an impurity charge of opposite sign to the actual charge $Z$. Consequently an aluminum vacancy with an effective charge of $-3$ is attracted to and repulsed by impurities having, respectively, a lower and higher valence than aluminum. Consequently, a monovalent copper atom dissolved in trivalent aluminum will attract a vacancy. The binding energy between the copper atom and the vacancy can be calculated using an asymptotic form of the oscillatory self-consistent Hartree potential.[39,40] The small binding energy of 0.05 eV determined in this computation could reduce the vacancy jump frequency $W_3$ away from a copper impurity atom by approximately 30% in the temperature range in which this experiment was carried out. Consequently, the ratio of $W_3/W_1$ of 0.30 for a dilute aluminum-copper alloy is reasonable if one accepts the proposition that either a very small impurity-vacancy binding energy and/or a slight loosening of the lattice around the undersized impurity has, respectively, reduced $W_3$ and increased $W_1$ from the vacancy jump frequency in pure aluminum.

Finally, the ratio of $W_3/W_1$ obtained from these experiments involving dilute aluminum-copper alloys is in accord with the ratios of $W_3/W_1$ at the same homologous temperature in other alloy systems. Table II lists the $W_3/W_1$ values found in dilute silver-zinc[1] and copper-zinc[2] alloys by Peterson and Rothman from measurements of the correlation coefficient and $W_3/W_1$ values for dilute aluminum-copper and aluminum-germanium[10] alloys determined by the method described in this paper.

TABLE II. The ratio of the vacancy jump frequency away from to that around an impurity atom in four dilute alloys at the same homologous temperature ($T/T_{\text{melt}} = 0.915$).

| Alloy System | Ag-Zn | Cu-Zn | Al-Cu | Al-Ge |
|---|---|---|---|---|
| $W_3/W_1$ | 0.37 | 0.90 | 0.30 | $>0.18$ |

## V. SUMMARY

During the cooling of a dilute aluminum-copper alloy from near its melting point, vacancies precipitated heterogeneously on the metal-oxide interface of the alloy and formed large vacancy condensation cavities. From the size of these cavities, the vacancy current which produced them could be directly determined. A microprobe examination in and around the vacancy condensation cavities determined the copper impurity current which had been generated by the vacancy current forming these cavities.

The ratio of the vacancy jump frequencies around and away from an impurity atom in a dilute fcc alloy was derived as a function of the impurity diffusion coefficient, the solvent diffusion coefficient, the vacancy current, and the impurity current generated by the vacancy current. From the ratio of vacancy and impurity currents established in this experiment and from diffusion coefficients available in the literature, the ratio of vacancy jump frequencies around and away from copper impurity atoms in aluminum was determined. This ratio reflects a small binding between a vacancy and a copper atom in aluminum and/or a slight increase in the jump frequency of solvent atoms next to the undersized copper impurity.

## ACKNOWLEDGMENT

I would like to thank R. H. Doremus for his critical review of the manuscript and for his suggestions, which helped to improve its presentation. This work was supported by the U. S. Army Research Office, Durham.

[1]S. J. Rothman and N. L. Peterson, Phys. Rev. 154, 552 (1967).

[2]N. L. Peterson and S. J. Rothman, Bull Am. Phys. Soc. 14, 389 (1969).

[3]R. E. Howard and J. R. Manning, Phys. Rev. 154, 561 (1967).

[4]S. R. deGroot and P. Mazur, *Non-Equilibrium Thermodynamics* (North-Holland, Amsterdam, 1962), p. 64.

[5]S. M. Hu, Phys. Rev. 180, 773 (1969).

[6]C. P. Flynn, Phil. Mag. 10, 909 (1964).

[7]R. E. Howard and A. B. Lidiard, Phil. Mag. 11, 1179 (1965).

[8]Equation (7) can be alternatively derived by comparing Eq. (5.1.42) of Ref. 9 with Eq. (2.17) of Ref. 7.

[9]R. E. Howard and A. B. Lidiard, Rept. Progr. Phys. 27, 161 (1964).

[10]T. R. Anthony, Acta. Met. 18, 307 (1970).

[11]R. E. Howard and A. B. Lidiard, J. Phys. Soc. Japan Suppl. 18, 197 (1963).

[12]N. L. Peterson and S. J. Rothman, Bull. Am. Phys. Soc. 12, 324 (1967).

[13]W. Alexander and L. M. Slifkin, Bull. Am. Phys. Soc.

14, 388 (1969).
[14]M. S. Anand and R. P. Agarwala, Trans. AIME 239, 1848 (1967).
[15]K. Hirano, R. P. Agarwala, and M. Cohen, Acta. Met. 10, 857 (1962).
[16]T. S. Lundy and J. F. Murdock, J. Appl. Phys. 33, 1671 (1962).
[17]S. P. Murarka, M. S. Anand, and R. P. Agarwala, Acta. Met. 16, 69 (1968).
[18]R. P. Agarwala, S. P. Murarka, and M. S. Anand, Acta. Met. 12, 871 (1964).
[19]M. S. Anand, S. P. Murarka, and R. P. Agarwala, J. Appl. Phys. 36, 3860 (1965).
[20]J. E. Hilliard, B. L. Averbach, and M. Cohen, Acta. Met. 7, 86 (1959).
[21]D. E. Ovsienko and I. K. Zasimchuh, Fiz. Metal. i Metalloved. 10, 743 (1960).
[22]M. Beyeler, thesis, University of Paris, 1968 (unpublished).
[23]T. Heuman and H. Böhmer, J. Phys. Chem. Solids 29, 237 (1968).
[24]T. J. Rowland and F. Y. Fradin, Phys. Rev. 182, 760 (1969).
[25]F. Y. Fradin and T. J. Rowland, Appl. Phys. Letters 11, 207 (1967).
[26]T. S. Lundy and J. F. Murdock, J. Appl. Phys. 33, 1671 (1962).
[27]T. G. Stoebe, R. D. Gulliver, T. O. Ogurtani, and R. A. Huggins, Acta. Met. 13, 701 (1965).
[28]P. E. Dougherty and R. S. Davis, Acta. Met. 7, 118 (1959).
[29]M. B. Kasen and D. H. Polonis, Acta. Met. 10, 821 (1962).
[30]J. R. Jasperse and P. E. Dougherty, Phil. Mag. 1, 635 (1964).
[31]B. K. Basu and C. Elbaum, Acta. Met. 13, 1117 (1965).
[32]M. B. Kasen, R. Taggart, and D. H. Polonis, Phil. Mag. 13, 453 (1966).
[33]D. Foss and O. H. Herbjørnsen, Phil. Mag. 13, 945 (1966).
[34]G. A. Chadwick, Phil. Mag. 14, 1295 (1966).
[35]O. H. Herbjørnsen and T. Astrup, Phil. Mag. 19, 693 (1969).
[36]T. R. Anthony, Acta. Met. 18, 471 (1970).
[37]B. K. Tarival and B. Ramaswami, J. Appl. Phys. (to be published).
[38]R. O. Simmons and R. W. Balluffi, Phys. Rev. 117, 52 (1960).
[39]S. M. Edelglass and M. Ohring, Trans. AIME 245, 186 (1969).
[40]A. Blandin, J. L. Déplanté, and J. Friedel, J. Phys. Soc. Japan Suppl. 18, 89 (1963).

PHYSICAL REVIEW B VOLUME 2, NUMBER 2 15 JULY 1970

# Infinite-$U$ Anderson Hamiltonian for Dilute Alloys*

G. Toulouse†

*Department of Physics, University of California at San Diego, La Jolla, California* 92037
(Received 15 December 1969)

A Hamiltonian corresponding to the strictly infinite-$U$ limit of the Anderson Hamiltonian is considered. It is argued that this Hamiltonian retains enough complexity to describe magnetic and nonmagnetic impurities. The relationships with the Kondo Hamiltonian are discussed. A resolvent formula for the T-matrix elements, convenient for diagram expansions, is given. The characterization and the summation of the most divergent terms for the susceptibility and the spin-flip T-matrix element, in the magnetic and nonmagnetic regimes, are carried out and shown to be much simpler than for the Kondo Hamiltonian.

## I. INTRODUCTION

The interest in the dilute alloy problem is now focused on the nature of the low-temperature solution for the Kondo Hamiltonian[1] and on the transition regime between magnetic and nonmagnetic behavior for the Anderson Hamiltonian.[2] Evidence is given here that the study of a Hamiltonian, corresponding to the $U \to \infty$ limit of the Anderson Hamiltonian, may shed some light on these two problems.

This Hamiltonian is[3,4]

$$H_M = \sum_{k\sigma} \epsilon_k n_{k\sigma} + E_d \sum_{\sigma} n_\sigma + V \sum_{k\sigma} (1 - n_{-\sigma})[c^\dagger_{k\sigma} c_\sigma + c^\dagger_\sigma c_{k\sigma}] \ .$$

It is easily seen that $[H_M, n_\uparrow, n_\downarrow] = 0$, so that there are two independent subspaces corresponding to $n_\uparrow n_\downarrow = 0$ and $n_\uparrow n_\downarrow = 1$; the subspace $n_\uparrow n_\downarrow = 0$ is such that the double occupation of the $d$ orbital is forbidden, which effectively corresponds to the limit $U \to \infty$.

For the full Anderson Hamiltonian, written in a transparent way as

$$H_A = h_0 + h_d + h_v + h_u \ ,$$

two typical choices of the perturbation term $H_1$ can be made.

(*a*) $H_1 = h_u$, *the Coulomb term.* In this case the umperturbed Hamiltonian is quadratic and standard